

Primary Structure, Ligand Binding, and Localization of the Human Type 3 Inositol 1,4,5-Trisphosphate Receptor Expressed in Intestinal Epithelium*

(Received for publication, June 22, 1993, and in revised form, September 1, 1993)

Anthony R. Maranto‡

From the Departments of Medicine and Biomedical Research, St. Elizabeth's Hospital of Boston, Tufts University School of Medicine, Boston, Massachusetts 02135

The second messenger, inositol 1,4,5-trisphosphate (InsP_3) transduces many hormonal signals which regulate Ca^{2+} -dependent processes in the intestinal epithelium. To study the receptors for InsP_3 (InsP_3Rs), which function as intracellular Ca^{2+} channels, cDNA clones encoding InsP_3Rs were isolated from a human colon adenocarcinoma cell line, HT29. The majority of clones encoded the type 3 InsP_3R , the product of the *ITPR3* gene on chromosome 6, for which only a 147-amino-acid fragment was known previously (Ozcelik, T., Sudhof, T. C., and Francke, U. (1991) *Cytogenet. Cell Genet. Abstr.* 58, 1880; Sudhof, T. C., Newton, C. L., Archer, B. T., III, Ushkaryov, Y. A., and Mignery, G. A. (1991) *EMBO J.* 10, 3199–3206). The complete sequence of the type 3 InsP_3R polypeptide (2,671 amino acids) is described here. Primary structure analysis indicates a pattern of conserved and variable regions which is characteristic of the InsP_3R family. A 250-kDa protein (SDS-PAGE) which specifically binds InsP_3 is immunoprecipitated by affinity-purified antibodies raised against a COOH-terminal fusion protein. Transient expression in COS-7 cells of a polypeptide comprising the NH₂-terminal 750 amino acids establishes that the ligand-binding domain is localized to this region. Lysates from transfected COS-7 cells bind InsP_3 with high affinity ($K_d = 151 \text{ nM}$) compared with other inositol phosphates ($\text{InsP}_3 >> \text{Ins } 1,3,4,5-\text{P}_4 > \text{InsP}_6 > \text{Ins } 1,4-\text{P}_2 >> \text{Ins } 1-\text{P}$). Immunocytochemical localization in the intestine reveals expression in crypt and villus epithelial cells, but not in cells of the lamina propria, submucosa, or muscularis layers. The subcellular distribution and appearance of staining is consistent with localization on the endoplasmic reticulum, with the highest concentration of staining occurring adjacent to the apical brush border of villus cells.

Inositol 1,4,5-trisphosphate receptors (InsP_3Rs)¹ constitute a family of Ca^{2+} channels which release Ca^{2+} from intracellular

* This work was supported by United States Public Health Service Grants DK44475 and P30 DK34928. The costs of publication of this article were defrayed in part by the payment of page charges. This article must therefore be hereby marked "advertisement" in accordance with 18 U.S.C. Section 1734 solely to indicate this fact.

† The nucleotide sequence(s) reported in this paper has been submitted to the GenBank™/EMBL Data Bank with accession number(s) V01062.

‡ To whom correspondence should be addressed: Box 93A, St. Elizabeth's Hospital, 736 Cambridge St., Boston, MA 02135. Tel.: 617-789-2678; Fax: 617-254-7488.

¹ The abbreviations used are: InsP_3R , InsP_3 receptor; InsP_3 , D-myo-inositol 1,4,5-trisphosphate; Ins 1-P, D-myo-inositol 1-monophosphate; Ins 1,4-P₂, D-myo-inositol 1,4-bisphosphate; Ins 1,3,4,5-P₄, D-myo-inositol 1,3,4,5-tetrakisphosphate; InsP_6 , D-myo-inositol hexakisphosphate; DMEM, Dulbecco's modified Eagle's medium; GST, glutathione S-transferase; PMSF, phenylmethylsulfonyl fluoride; TBS, Tris-buffered saline; PBS, phosphate-buffered saline; PCR, polymerase chain

reservoirs in response to the second messenger InsP_3 (1–6). InsP_3Rs are encoded by several related genes. Complete cDNA sequences are available for mouse, rat, and *Xenopus* type 1 InsP_3Rs (2–4), rat type 2 InsP_3R (5), and a *Drosophila* InsP_3R (6). Only partial sequences for human and mouse type 3 InsP_3Rs (5, 7) and mouse type 4 InsP_3R (7) have been reported. Alternatively spliced subtypes of the type 1 InsP_3R have also been detected (3, 8, 9). Among various tissues, InsP_3R mRNAs are differentially expressed (3, 7) and differentially spliced (8, 9), suggesting that specific forms of InsP_3Rs may be functionally specialized.

Studies with the type 1 InsP_3R isolated from the cerebellum indicate that the InsP_3R molecule may represent a point where the Ca^{2+} -signaling pathway is modulated by other second messenger pathways. The type 1 InsP_3R is phosphorylated by cAMP-dependent protein kinase (10), protein kinase C (11), and Ca^{2+} /calmodulin-dependent protein kinase II (11). In addition, ATP (12, 13) and calmodulin (13) bind to this receptor with high affinity.

Cytosolic Ca^{2+} mobilization mediates the effects of a subset of neurotransmitters (14–16), hormones (17, 18), and inflammatory agents (14, 19) which act on intestinal epithelial cells. In enterocytes, as in most other types of cells, occupation of plasma membrane receptors activates phospholipase C to produce InsP_3 (16–18) which then releases Ca^{2+} from intracellular stores (20–23). Once released, Ca^{2+} acts on a variety of effectors in enterocytes. In crypt cells, Ca^{2+} activates basolateral K^+ channels to hyperpolarize the plasma membrane and potentiate Cl^- secretion through cAMP-regulated Cl^- channels (24). Ca^{2+} also appears to open a separate class of Cl^- channels via activation of Ca^{2+} /calmodulin-dependent protein kinase II (25). In villus enterocytes, Ca^{2+} activation of Ca^{2+} /calmodulin-dependent protein kinase II inhibits Na^+/H^+ exchange across the apical membrane (26). In addition to modulating ion transport, Ca^{2+} may also regulate cytoskeletal interactions in the villus and terminal web regions. Recently, Ca^{2+} /calmodulin-dependent protein kinase II has been found to be tightly associated with cytoskeletal components of the terminal web (27). Also, Ca^{2+} causes the dissociation of the myosin I-calmodulin complex which is the major component of the cross-bridges that connect actin to the microvillus membrane (28).

Clearly, to understand how InsP_3 and other second messengers regulate Ca^{2+} release and mediate such diverse effects, it is necessary to study the molecular properties and intracellular localization of InsP_3Rs in enterocytes. The HT29 cell line (29), derived from a human colon adenocarcinoma, is an attractive preparation for studying enterocyte InsP_3Rs for several reasons. (a) Since it is an established cell line, the contamination by lymphoid and smooth muscle cells in isolated intestinal

reaction; PAGE, polyacrylamide gel electrophoresis.

tissue is avoided. (b) HT29 cells express receptors for a number of hormones and growth factors (30), some of which stimulate InsP₃ production and Ca²⁺ mobilization (17, 25), indicating that the InsP₃-signaling pathway is intact. (c) HT29 cells continue to divide and express an undifferentiated phenotype when cultured in the presence of glucose, but terminally differentiate into enterocyte-like and goblet-like cells when glucose is substituted with another carbon source (31). Since their differentiation can be modulated, HT29 cells could prove to be useful for studying transcriptional regulation of InsP₃R genes during differentiation.

Therefore, to initiate a study of the InsP₃Rs which are expressed in enterocytes, cDNA clones encoding InsP₃Rs were isolated from a library derived from HT29 cells. The majority of clones encoded the type 3 InsP₃R, the product of the *ITPR3* gene on chromosome 6 (32), for which only a 147-amino-acid fragment was known previously (5). Here, the complete amino acid sequence of the human type 3 InsP₃R is reported. Its characterization by immunoprecipitation, functional expression, ligand binding, and immunocytochemical localization is also described.

EXPERIMENTAL PROCEDURES

Materials—[α -³²P]dATP (3000 Ci/mmol) was from ICN. [³H]InsP₃ (17 Ci/mmol) was from DuPont-New England Nuclear. Nonradioactive inositol phosphates were from Calbiochem. DNA modifying enzymes were from New England Biolabs and United States Biochemical. Glutathione-agarose, protein A-Sepharose, and Dulbecco's modified Eagle's medium (DMEM) were from Sigma. Cell lines HT29 and COS-7 were from the American Type Culture Collection.

cDNA Cloning—A cDNA library was constructed and provided as a gift by N. E. Simister, Brandeis University, Waltham, MA. Briefly, double-stranded cDNA was synthesized with poly(A)⁺RNA from undifferentiated HT29 cells as template and oligo(dT) as primer. The cDNA was methylated with EcoRI methylase, blunted, ligated with an EcoRI linker, digested with EcoRI, and fractionated by agarose gel electrophoresis. Sequences longer than 2 kilobase pairs were ligated into the EcoRI site of λ -gt11. An estimated 2×10^{10} independent recombinant phage were produced.

Initial InsP₃R cDNA clones were identified by screening 2×10^6 phage plaques with a ³²P-labeled cDNA probe encoding the last putative transmembrane region of the mouse cerebellar InsP₃R (2). The probe was constructed by PCR amplification of mouse brain cDNA with synthetic oligonucleotides AAGGATCTGCTCCCTGCCGAAGAAC and CCGGATCCAAGCCGCAGATGAAGCAC to generate a product containing 310 base pairs of coding sequence bounded by EcoRI sites. The product was digested with EcoRI, inserted into the EcoRI site of the plasmid pGEM-3Z (Promega), and verified by sequencing. Labeled probe was prepared by the incorporation of [α -³²P]dATP during random-primed DNA synthesis using this re-excised insert as a template. Hybridization was performed for 16 h at 60 °C in a buffer containing 2 × SSC, 7% SDS, 0.5% nonfat dry milk, 0.1 mg/ml herring sperm DNA, and ³²P-labeled probe (8.75×10^5 cpm/ml). Filters were washed at 60 °C in two 20-min changes of low stringency buffer containing 1 × SSC and 0.1% SDS. Subsequent screenings were performed with probes generated from 5' restriction fragments of positive clones.

cDNA Sequencing—Phage from positive plaques were amplified in large scale liquid lysates and purified by CsCl gradient centrifugation. Their cDNA inserts were excised with EcoRI, purified by agarose gel electrophoresis and glass bead capture, and recloned into pGEM-3Z for restriction mapping. Shorter templates for sequencing were prepared by subcloning nested restriction fragments into pGEM-3Z. Sequencing of denatured, double-stranded DNA was performed by the dideoxy chain termination method (33) using Sequenase II (United States Biochemical) and M13, SP6, or sequence-specific oligonucleotide primers. Both strands were completely sequenced.

Production of Fusion Protein and Affinity-purified Anti-fusion Protein Antibodies—A fusion protein was created which contained the GST of the pGEX bacterial expression vector and the COOH-terminal 27 amino acids of the type 3 InsP₃R (Figs. 1C and 3B). The expression vector was constructed as follows. The *SacI*(7973)/*SacI*(vector) fragment of p23 (Fig. 1A) was ligated into the *SacI* site of pGEM-3Z to yield p23a2. This insert was excised by digestion of the flanking vector *EcoRI* sites and ligated with *EcoRI*-linearized pGEX-1 (Pharmacia LKB Bio-

technology Inc.) to produce a coding sequence which was in frame with the GST coding sequence of pGEX-1. Following transformation of *Escherichia coli* (JM109), correctly oriented constructs were identified by restriction mapping. Fusion protein was produced by growing bacterial transformants into log phase and inducing with 1 mM isopropyl- β -D-thiogalactopyranoside for 3 h at 37 °C. Cells were collected by centrifugation and lysed by sonication on ice in PBS containing 1% Triton X-100, 100 mM EDTA, and 1 mM PMSF. Following clearing by centrifugation at 10,000 × g for 10 min, the supernatant was incubated with glutathione-agarose beads for 5 min on ice. The beads were washed twice with ice-cold PBS, and the fusion protein was eluted by adding 10 mM reduced glutathione in 50 mM Tris-Cl, pH 8.0. Glutathione was removed by dialysis against PBS overnight at 4 °C. The presence of the expected 30-kDa fusion protein, termed GST-H3CT, was verified by SDS-PAGE.

Female New Zealand White rabbits were injected intradermally with 500 µg of GST-H3CT emulsified with Freund's complete adjuvant. At 4-week intervals thereafter, rabbits were boosted with 200 µg of GST-H3CT in Freund's incomplete adjuvant. Antibodies recognizing GST-H3CT were detectable by Western blotting beginning 2 weeks after the first booster injection.

Anti-GST-H3CT antibodies were affinity-purified from serum using purified GST-H3CT coupled to Affi-Gel 10 (Bio-Rad). Following batch incubation with serum for 2 h at room temperature, the affinity matrix was extensively washed with 1 M guanidinium HCl followed by 50 mM Tris-HCl, pH 7.4. Specific antibodies were eluted from the matrix with 4.5 M MgCl₂ in 50 mM Tris-HCl, pH 7.4, containing 0.1% bovine serum albumin. The eluted antibodies were dialyzed against PBS for 3 h and against PBS containing 35% glycerol and 0.02% sodium azide overnight at 4 °C. Antibodies were stored at 4 °C.

Preparation of Cell Extracts and Immunoprecipitations—HT29 cells were cultured at 37 °C in DMEM supplemented with 4500 mg/liter glucose and 10% newborn calf serum in an atmosphere containing 5% CO₂, 95% air at 100% humidity. Under these conditions, these cells continue to divide after reaching confluence (about 5 days after plating 1:5) and remain largely undifferentiated. Cells were lysed directly in 100-cm culture dishes 7–10 days after plating as follows. Each dish of PBS-washed cells received 1 ml of lysis buffer containing 50 mM Tris-HCl, pH 7.5, 1% Triton X-100, 150 mM NaCl, 1 mM EDTA, and 1 mM PMSF. Lysed cells were scraped from the dishes and homogenized on ice for 10 min in a Dounce-type homogenizer. Lysates were precleaned by incubation with protein A-Sepharose for 1 h at 4 °C followed by centrifugation at 15,000 × g for 5 min. The protein concentration was determined using a bicinchoninic acid assay (Pierce Chemical Co.) and adjusted to 1 mg/ml by the addition of lysis buffer.

Immunoprecipitations were performed by incubating 500 µl of cell lysate with 50 µl of anti-GST-H3CT affinity-purified antibodies on ice for 2 h. Complexes were precipitated by adding 100 µl of a 1:1 slurry of protein A-Sepharose in lysis buffer, incubating 1 additional hour, and pelleting at 15,000 × g for 1 min. Immunoprecipitates were washed three times with 1 ml of lysis buffer and subjected to InsP₃ binding studies or SDS-PAGE and Western blotting as described below. Controls were treated exactly as above except that 50 µl of lysis buffer or 50 µl of preimmune rabbit serum were substituted for the affinity-purified antibodies.

Expression of the Ligand-binding Domain of the Type 3 InsP₃R by Transfection—The mammalian expression plasmid pSVL-HUMIP3R3Δ751–2593 uses the SV40 late promoter to drive the expression of a mutant type 3 InsP₃R in which the NH₂-terminal 750 residues (containing the putative InsP₃-binding domain) are fused to the COOH-terminal 78 residues (containing the epitopes recognized by anti-H3CT antibodies) (Fig. 1D). The plasmid was constructed as follows (see Fig. 1A for restriction sites). A PCR fragment including the translation start ATG triplet was generated by amplification of the first 224 base pairs of cDNA from clone p313 with synthetic oligonucleotides AATCTAGAC-GCCCCCACGCCCTG and AGAATTCAATGGGGCACACCTTGAG. The *Xba*I and *Eco*RI sites created at the ends of the product were digested, and the fragment was ligated with the *Xba*I/*Eco*RI fragment from pGEM-3Z to yield p313S1. The *Sac*II(158)/*Eco*RI(vector) fragment containing pGEM-3Z from p313S1 was ligated with the 2.4-kb *Sac*II(158)/*Eco*RI(vector) fragment from p313 to yield p313S2. The *Kpn*I(2229)/*Eco*RI(vector) fragment containing pGEM-3Z from p313S2 was ligated with the 4.7-kb *Kpn*I(2229)/*Eco*RI(vector) fragment from p203 to yield p313S2–203. The 6.7-kb *Xba*I(vector)/*Bam*HI(6767) fragment from p313S2–203 was ligated with the *Xba*I/*Bam*HI fragment from pSVL (Pharmacia) to yield pSVL-313S-203. The fragment encoding the COOH-terminal was prepared by ligating the *Ava*I(7511)/*Ava*I(8127) fragment from p23 with *Ava*I-digested pGEM-3Z to yield

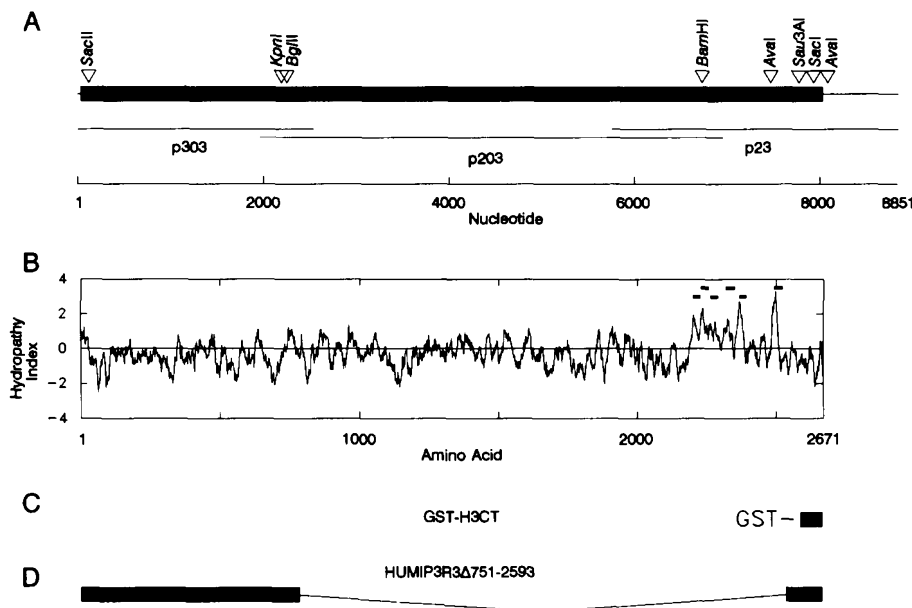


FIG. 1. Structures of the type 3 InsP_3R cDNA and the expression constructs used in this study. *A*, the positions of the three cDNA clones (*p303*, *p203*, *p23*) which were sequenced to yield the complete coding region (black bar) are shown. Restriction sites used to synthesize the expression constructs in *C* and *D* are also indicated. *B*, hydropathy plot of the deduced amino acid sequence computed with a window size of 20 amino acids according to the method of Kyte and Doolittle (53). Six putative transmembrane segments are indicated by black bars. *C*, structure of the bacterial fusion protein GST-H3CT used in the production of anti-fusion protein antiserum. A cDNA fragment encoding the COOH-terminal 27 amino acids of the type 3 InsP_3R was fused in frame to the GST gene in pGEX-1. *D*, structure of the mutant construct, HUMIP3R3Δ751-2593, which was expressed in COS-7 cells to characterize the binding of inositol phosphates to the ligand binding domain. cDNA fragments encoding the first 750 and last 78 amino acids of the type 3 InsP_3R were fused in-frame and inserted after the SV40 late promoter sequence in pSVL.

p23a6. Finally, the *Bgl*II(2285)/*Bam*HI(6767) fragment from pSVL-313S2-203 was excised and replaced with the 0.3-kb *Sau*3A(7814)/*Bam*HI(vector) fragment from *p23a6* to yield pSVL-HUMIP3R3Δ751-2593.

The mutant type 3 expression plasmid or pSVL vector as a control were transfected into COS-7 cells as follows. Cells were incubated for 3 h at 37 °C in DMEM containing 10% NuSerum (Collaborative Research), 400 µg/ml DEAE-dextran, 100 µM chloroquine, and 1 µg/ml plasmid DNA. Following incubation, cells were treated for 2 min with 10% dimethyl sulfoxide in PBS, rinsed with PBS, then allowed to grow 48–72 h in DMEM containing 10% newborn calf serum. Expression was monitored with immunofluorescence using anti-GST-H3CT antibodies to label parallel cultures of transfected cells grown on coverslips. To harvest protein, cells were lysed with buffer containing 50 mM Tris-HCl, pH 8.3, 1% Triton X-100, 1 mM EDTA, and 1 mM PMSF, then homogenized for 10 min on ice, and centrifuged for 5 min at 15,000 × *g*. Supernatants were used for InsP_3 binding and Western blotting studies.

SDS-PAGE and Western Blotting—Lysates or immunoprecipitates were mixed with Laemmli sample buffer (34) and separated on 5–15% polyacrylamide gradient gels containing 0.1% SDS. Proteins were transferred electrophoretically to nitrocellulose in Towbin buffer (35). The resulting Western blots were blocked for 1 h with 5% non-fat dry milk in TBS. Primary antibodies were diluted in the same buffer and allowed to bind overnight at 4 °C. Immunoreactive bands were visualized by incubating the washed blots with protein A-horseradish peroxidase conjugate (Bio-Rad) which was detected with an enhanced chemiluminescence system (Amersham Corp.).

InsP_3 Binding Assays—Binding assays were performed in 150 µl of binding buffer containing 50 mM Tris-HCl, pH 8.3, 1% Triton X-100, 1 mM EDTA, and 100 µg of protein. The final concentration of [^3H] InsP_3 in all assays was 8 nM. Nonspecific binding was measured by the addition of 2 µM unlabeled InsP_3 to half of the reactions. After equilibration for 5 min on ice, samples received 50 µl of 5 mg/ml γ -globulin and 100 µl of 25% polyethylene glycol 8000. Following an additional 5 min equilibration on ice, the samples were centrifuged at 15,000 × *g* for 5 min to pellet the aggregated protein containing the ligand-receptor complexes. The pellets were rinsed once with 1 ml of ice-cold binding buffer, resuspended with 0.1 N NaOH, and their radioactivity was measured by liquid scintillation counting. Competitive binding studies to measure the binding affinity of InsP_3 or the IC_{50} values of other inositol phosphates were performed exactly as above except that samples also contained serial dilutions of these inhibitors.

Immunocytochemical Studies—Frozen 10-µm sections of rat jejunum

were prepared with a cryostat and collected on gelatin-coated slides. Sections were fixed for 20 min at -20 °C in methanol, rehydrated with TBS, and blocked with TBS containing 2% goat serum. Affinity-purified anti-GST-H3CT antibodies (1:100–1:500) were added to the blocking buffer and allowed to react overnight at 4 °C. Control sections were incubated with the fraction of anti-GST-H3CT antiserum which bound to an affinity matrix of only the GST carrier protein. Preimmune sera were not useful as controls because of the presence of antibodies which labeled multiple cellular structures. Following primary labeling, sections were washed with three changes of TBS for 5 min each and then incubated with rhodamine-conjugated goat anti-rabbit antibodies (Boehringer Mannheim, 1:200 in blocking buffer) for 2 h at room temperature. Sections were washed three times with TBS and mounted in 50% glycerol in TBS.

RESULTS

Cloning of Type 3 InsP_3R cDNA—Of the six clones that were identified by the initial screening, five were judged as encoding the type 3 InsP_3R because their translations included a fragment of the type 3 InsP_3R which had been previously isolated from a human kidney cDNA library by PCR cloning (5). The remaining clone was judged as encoding the human homolog of the type 1 InsP_3R because a translation of 533 amino acids shared 96% identity with rodent type 1 InsP_3Rs (2, 3). Clones encoding the remainder of the type 3 InsP_3R were isolated in two subsequent screenings using restriction fragments from the 5' ends of the longest clones as probes. A total of 12 type 3 InsP_3R clones were isolated. The sequence of the entire receptor was determined by completely sequencing three of these overlapping clones as follows (Fig. 1A): p313 (nucleotides 1–2572), p203 (1994–6991), and p23 (5786–8851). Restriction maps of the nine clones which were not completely sequenced were in perfect register with the maps of these three overlapping clones, suggesting that alternatively spliced variants were not present among the 12 clones.

The longest open reading frame begins at nucleotide 37 and continues until nucleotide 8050 where a TGA termination codon occurs (Fig. 2). The sequence surrounding the first Met codon, GCCGCAGCCATGA, provides a favorable context for

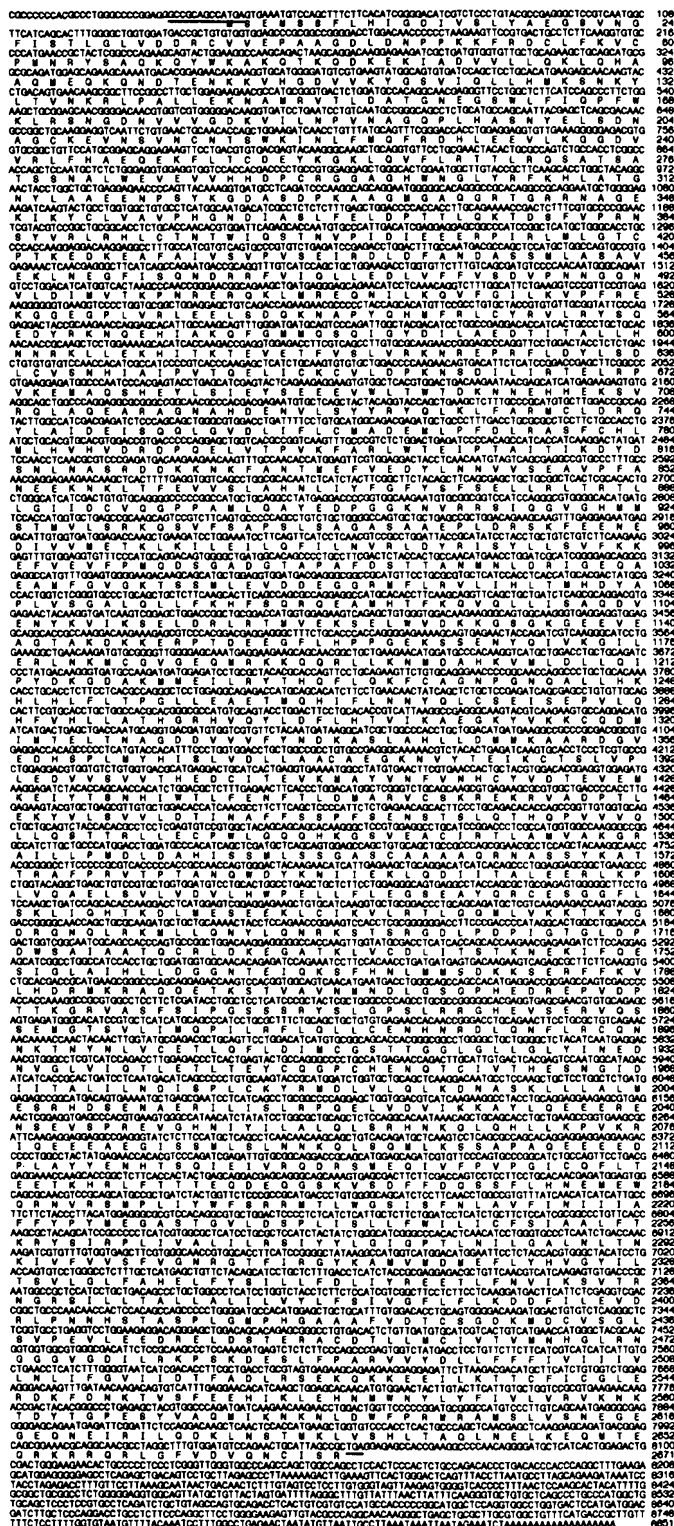


FIG. 2. Nucleotide and predicted amino acid sequences of the human type 3 InsP_3R . The sequences are numbered at the right. The translation initiation consensus sequence, termination codon, and polyadenylation consensus sequence are *underlined*.

initiation: a purine is positioned three bases upstream of the ATG and all but two nucleotides match the consensus sequence for initiation, GCCGCC(A/G)CCATGG , reported by Kozak (36). The 3'-untranslated region contains a polyadenylation signal, AATAAA , which is followed 13 bases later by a poly(A) tail.

The length of the cDNA (8,851 bases) is less than the size of the message (9,400 bases) estimated from Northern blots (data

not shown). The short 5'-untranslated region suggests that the 5' leader sequence of the mRNA may be longer than shown here. Rapid amplification of the cDNA 5' end (5'-RACE) was attempted to obtain more 5' sequence, but was unsuccessful. However, the NH_2 -terminal region of a translation beginning at the first Met codon is almost identical to the NH_2 -termini of all other known InsP_3R sequences (Fig. 3A), suggesting that the complete coding region of the type 3 InsP_3R was cloned.

Protein Structure and Comparisons with Other InsP_3Rs

The open reading frame encodes a sequence of 2,671 amino acids with a calculated M_r of 304,112 Da. Hydrophobicity analysis suggested that the type 3 InsP_3R shares a similar topology with other InsP_3Rs : at the NH_2 -terminal end, a large hydrophilic region comprising 80% of the protein is followed by a cluster of hydrophobic segments and a short hydrophilic COOH-terminal (Fig. 1B). Using two independent algorithms for predicting transmembrane helices (37, 38), six putative transmembrane segments were identified: residues 2203–2223, 2231–2255, 2264–2288, 2320–2350, 2369–2391, 2494–2520. In this tentative model, the large NH_2 -terminal and small COOH-terminal regions are on the cytoplasmic side of the membrane while a large loop between the fifth and sixth transmembrane segments is on the opposite side. The topology predicted here agrees with predictions for the homologous transmembrane domains of the mouse and *Xenopus* type 1 (2, 4) and *Drosophila* (6) InsP_3Rs . An alternative model with eight transmembrane-spanning segments has also been proposed for the rat type 1 (3) and type 2 (5) InsP_3Rs . Final assignments for all of these sequences await biochemical confirmation.

Dot matrix protein comparisons of the type 3 InsP_3R with other InsP_3Rs revealed further details of a common structural organization (Fig. 3C). No internal repeats were detected when the type 3 sequence was compared with itself. Intersequence comparisons demonstrated a conserved pattern among the sequences consisting of several long regions of similarity separated by short divergent regions. Furthermore, the arrangement of these regions was not dependent on the choice of the sequence used along the abscissa. Based on dot matrix observations and sequence alignments, 13 conserved and 13 variable regions can be delineated. Their locations are indicated along the type 3 InsP_3R diagram in Fig. 3D. The lengths of the conserved regions range between 42 and 325 amino acids, while the lengths of the variable regions range between 10 and 63 amino acids. There is a considerable degree of similarity between the homologous conserved regions of all known InsP_3Rs . Comparing conserved regions between the human type 3 and rat type 1 InsP_3Rs , the percentages of identical amino acids range between 62 and 83%. A complete list of similarity comparisons for the conserved regions of these two isoforms may be found in Table I.

Deletions and insertions are present in the type 3 sequence relative to the other InsP_3R sequences. Most of these differences are located within or at the borders of the variable regions. Relative to the known alternatively spliced subtypes of the type 1 receptor (3, 8, 9), in the type 3 receptor, a deletion of 15 residues from the first variable region does not occur, but a deletion of 40 residues from the eighth variable region does occur. An additional relative deletion of 27 residues occurs in the ninth variable region of the type 3 InsP_3R and an insertion of 31 residues is present in the 10th variable region (Fig. 3D).

The type 1 InsP_3R is a major substrate for phosphorylation by cAMP-dependent protein kinase in the cerebellum (2). *In vitro*, cAMP-dependent protein kinase phosphorylates the type 1 receptor at 2 Ser residues in the large cytoplasmic region (39). These sites are within variable regions and have not been conserved in the type 3 InsP_3R . However, five different PKA phosphorylation consensus sites ($\text{Arg/Lys-Arg/Lys-Xaa-Ser/Thr}$)

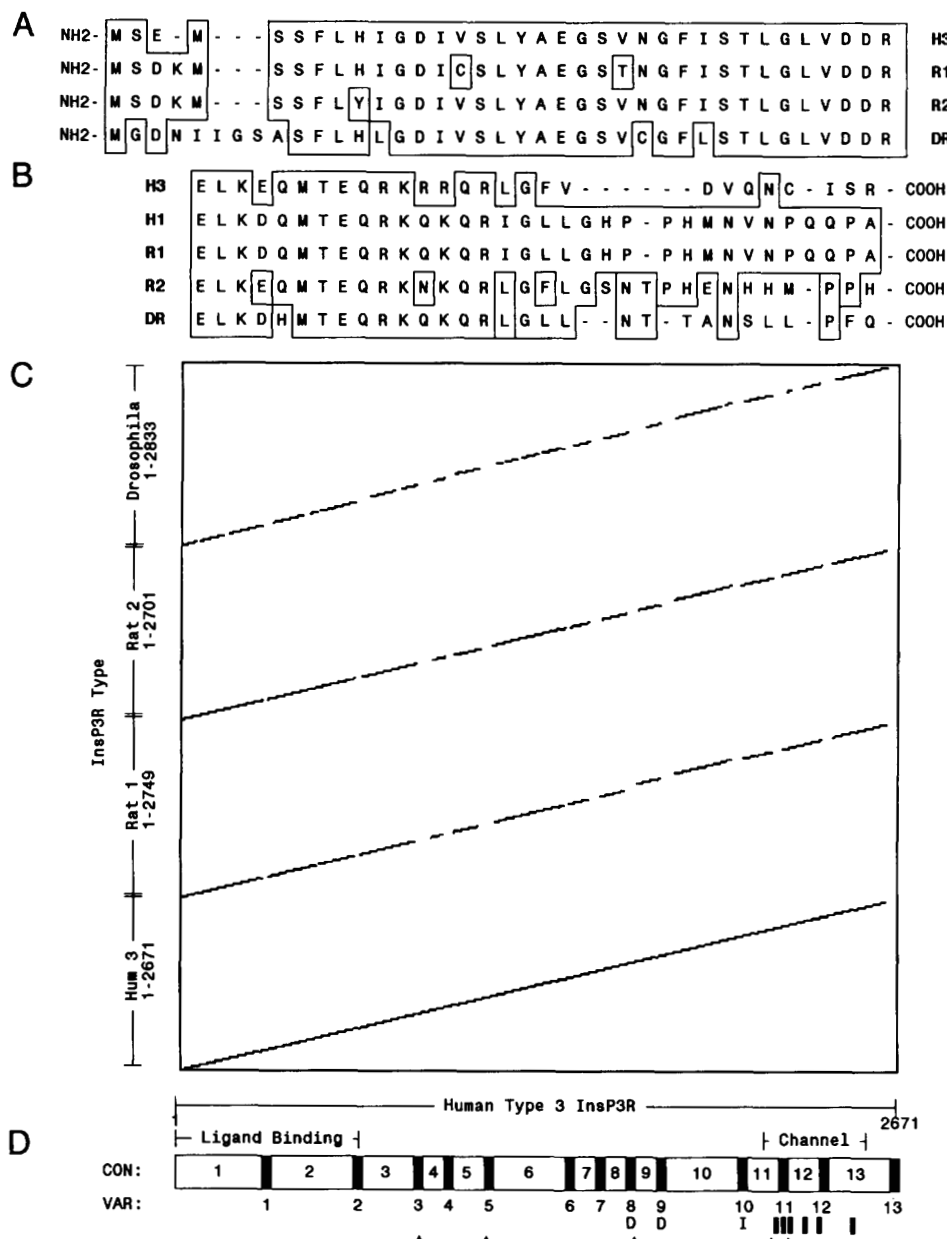


FIG. 3. Comparison of the amino acid sequences of the type 3 InsP₃R and other InsP₃R types. *A*, alignment of the NH₂-terminal sequences of the human type 3 InsP₃R (*H3*), rat type 1 InsP₃R (*R1*) (3), rat type 2 InsP₃R (*R2*) (5), and *Drosophila* InsP₃R (*DR*) (6). *B*, alignment of the COOH-terminal 27 amino acids of the type 3 InsP₃R (*H3*) with the COOH-terminal sequences of the human type 1 InsP₃R (*H1*), which was also cloned here from the HT29 cDNA library, and other reported InsP₃R types (*R1*, *R2*, *DR*) (3, 5, 6). Antiserum raised against the fusion protein GST-H3CT, containing this 27 amino acid sequence of the type 3 InsP₃R did not cross-react with rat or human type 1 InsP₃R (data not shown). *C*, dot matrix comparison of the amino acid sequence of the type 3 InsP₃R with other InsP₃R sequences using the program DOTPLOT, by R. C. Nakisa (available via anonymous ftp from ftp.bio.indiana.edu). The dots correspond to the mid-points of 40-residue windows in which 15 residues are identical. In the type 3 receptor self-comparison (bottom diagonal), the absence of other diagonals indicates the absence of internal repeats. Comparisons with the other sequences reveal an organization in which highly similar regions (diagonal lines) are separated by short divergent regions (gaps). This pattern of similar and divergent regions does not change appreciably when each of the other InsP₃R types are used as the abscissa (not shown), indicating that these regions are constant features of InsP₃R types. *D*, summary of the architecture of InsP₃R types. Evidence presented in this and other studies (44, 45) suggests that the InsP₃-binding and Ca²⁺-channel domains reside in the NH₂- and COOH-terminal regions, respectively. Superimposed on this model are 13 conserved (CON:1-13, clear boxes) and 13 variable (VAR:1-13, filled boxes) regions deduced from the dotplot in *B*. Relative to the long form of the rat type 1 InsP₃R (3), deletions (D) of 40 residues and 27 residues occur in the eighth and ninth variable regions, respectively. An insertion (I) of 31 residues is present in the tenth variable region. Also shown are the locations of the six putative transmembrane segments (vertical bars) and five cAMP-dependent protein kinase phosphorylation consensus sequences (arrowheads) of the type 3 receptor.

(40) are present in the type 3 InsP₃R (Fig. 3*D*). Three of these sites (Ser-934, Ser-1133, Thr-1701) are in variable regions in the midportion of the sequence. The other two sites (Thr-2202, Ser-2260) are positioned at the cytoplasmic end of the first and third transmembrane segments, suggesting possible roles in regulating the activity of the Ca²⁺ channel. The type 1 InsP₃R

can also be phosphorylated *in vitro* by protein kinase C and Ca²⁺/calmodulin-dependent protein kinase II (11). The type 3 InsP₃R contains 18 potential phosphorylation sites for protein kinase C (Ser/Thr-Xaa-Arg/Lys)(41) and 16 possible sites for Ca²⁺/calmodulin-dependent protein kinase II (Arg-Xaa-Xaa-Ser/Thr) (42), but the physiological significance of these sites

TABLE I

Comparison of the conserved regions of the human type 3 and rat type 1 InsP_3R

Conserved regions were identified by dot matrix analysis as in Fig. 3C. Percent amino acid identity and similarity were determined by aligning the amino acid sequences. Similarities were judged as follows: A,S,T; D,E; N,Q; R,K; I,L,M,V; F,Y,W. The rat type 1 InsP_3R sequence was obtained from Ref. 3.

Conserved region	Residue range		% identity	% similarity
	Type 3 InsP_3R	Type 1 InsP_3R		
1	1–318	1–317	79	7
2	345–670	346–670	72	11
3	689–895	693–898	71	9
4	958–1000	961–1003	79	12
5	1028–1130	1033–1135	69	15
6	1168–1452	1171–1462	68	15
7	1479–1545	1490–1556	63	12
8	1587–1682	1596–1692	70	13
9	1725–1812	1795–1882	63	11
10	1869–2073	1964–2175	83	4
11	2111–2224	2182–2295	62	16
12	2272–2404	2343–2475	73	14
13	2452–2661	2524–2732	82	10

remains to be demonstrated.

Immunoprecipitation of the Native Receptor with Anti-fusion Protein Antibodies—To develop an antiserum which would recognize only the type 3 receptor, the cDNA was used to create a fusion protein which contained the COOH-terminal 27 amino acids of the type 3 InsP_3R fused to the GST encoded by the pGEX bacterial expression vector (Fig. 1C). This region was chosen because the COOH-terminal sequence of the type 3 InsP_3R was found to be divergent relative to the human type 1 InsP_3R sequence also cloned here and to the other reported InsP_3R sequences (2–6) (Fig. 3B). Rabbits were immunized with the fusion protein, GST-H3CT, and antibodies were purified on a GST-H3CT affinity matrix. The affinity-purified antibodies were used to immunoprecipitate native type 3 InsP_3R from HT29 cell lysates and to detect the receptor by Western blotting. The antibodies detected a single 250 kDa band in control supernatants treated with buffer alone or with rabbit preimmune serum, and this protein was significantly depleted from the supernatant by the addition of anti-GST-H3CT antibodies (Fig. 4A, center panel). Addition of anti-GST-H3CT antibodies also depleted 65% of the specific [^3H]InsP₃-binding activity from the supernatant, while the addition of preimmune serum had no effect on binding (Fig. 4A, right panel). When the immunoprecipitates were analyzed, a single 250 kDa band was detected by Coomassie Blue staining (Fig. 4B, left panel) and by Western blotting (Fig. 4B, center panel). In parallel, [^3H]InsP₃ binding activity was recovered in the anti-GST-H3CT precipitate but not in the controls (Fig. 4B, right panel).

An antiserum raised against a 19-residue COOH-terminal peptide of the type 1 InsP_3R (a gift from P. DeCamilli, Yale University, New Haven, CT) did not react with the anti-GST-H3CT precipitate. However, this antiserum did detect a 260 kDa band present in HT29 lysates (data not shown), suggesting that type 1 and type 3 InsP_3Rs have slightly different electrophoretic mobilities and that these two antisera are specific for their respective receptors.

It is noteworthy that the apparent molecular mass of the type 3 InsP_3R by SDS-PAGE is approximately 50 kDa less than the molecular mass predicted from sequencing data. Other InsP_3Rs migrate in a similar anomalous manner by SDS-PAGE (2–6). To examine the possibility that post-translational proteolytic processing might be accounting for this discrepancy, the 250 kDa band which was immunoprecipitated by anti-GST-H3CT was transferred to Immobilon P (Millipore) (43) and

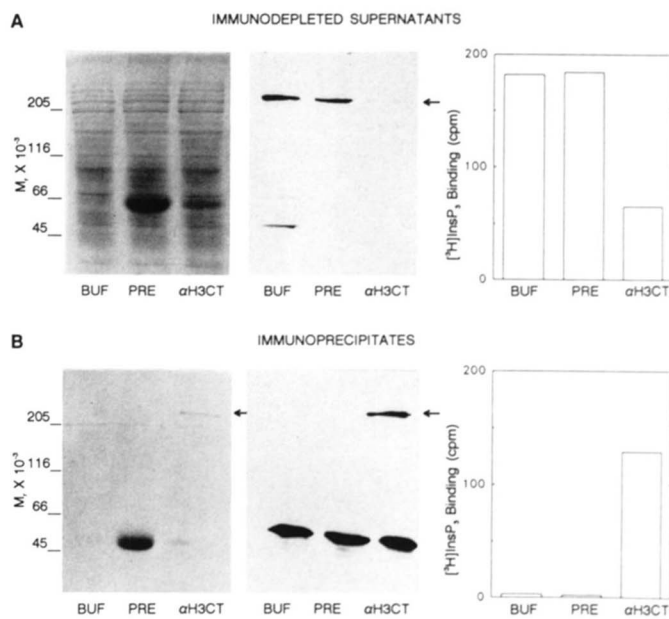


FIG. 4. Western blot and $[^3\text{H}]$ InsP₃ binding analyses of a 250-kDa protein immunoprecipitated from HT29 cell lysates by anti-GST-H3CT antibodies. HT29 cell lysates were immunoprecipitated with anti-fusion protein GST-H3CT antibodies (α H3CT) or controls: buffer (BUF), preimmune serum (PRE) as described below. A, analysis of immunodepleted supernatants by: left panel, Coomassie Blue staining following SDS-PAGE (50 $\mu\text{g}/\text{lane}$); middle panel, Western blot of a companion gel labeled with anti-GST-H3CT antibodies (50 μg protein/lane); right panel, specific binding of [^3H]InsP₃ (100 μg protein/assay). The disappearance of the 250 kDa band caused by immunodepletion with anti-GST-H3CT antibodies is indicated by an arrow. B, corresponding immunoprecipitates analyzed by Coomassie Blue staining (left), Western blotting (middle), and [^3H]InsP₃ binding (right). For electrophoresis, immunoprecipitates from 150 μg initial lysate protein were loaded in each lane. The 250 kDa band is evident in the anti-GST-H3CT immunoprecipitate lanes of the stained gel and the immunoblot (arrows). For [^3H]InsP₃ binding, the data have been normalized to represent the amount of binding activity precipitated from lysate containing 100 μg protein. Binding data are means of duplicate determinations. Immunoprecipitations were repeated three times with similar results.

analyzed by automated Edman degradation and acid hydrolysis for amino acid sequence and composition determination, respectively. NH₂-terminal blockage prevented sequencing, but the amino acid analysis agreed well with the predicted amino acid composition (data not shown), indicating that aberrant electrophoretic mobility rather than post-translational cleavage probably accounts for the discrepancy between the predicted and apparent M_r .

Expression of the Ligand-binding Domain—Previous studies demonstrated that expression of the NH₂-terminal fourth of the type 1 InsP_3R was sufficient to produce InsP₃ binding activity (44, 45). In the homologous portion of the type 3 InsP_3R described here, except for a 26-residue variable region, 76% of the amino acids are perfectly conserved and 9% are functionally conserved relative to the type 1 receptor. This similarity suggested that this region of the type 3 InsP_3R might also constitute the ligand-binding domain. To test this hypothesis, a cDNA fragment encoding the NH₂-terminal 750 residues of the type 3 receptor was transiently expressed in COS-7 cells. A fragment of cDNA encoding the COOH-terminal 78 residues was fused in-frame to the NH₂-terminal fragment (Fig. 1D) to enable detection of recombinant protein expression using the anti-GST-H3CT antiserum which reacts with the COOH-terminal. This construct was efficiently transfected into COS-7 cells and caused high levels of recombinant protein expression as demonstrated by immunofluorescence (Fig. 5, A and B) and Western blotting (Fig. 5C). Lysates from cells transfected with the

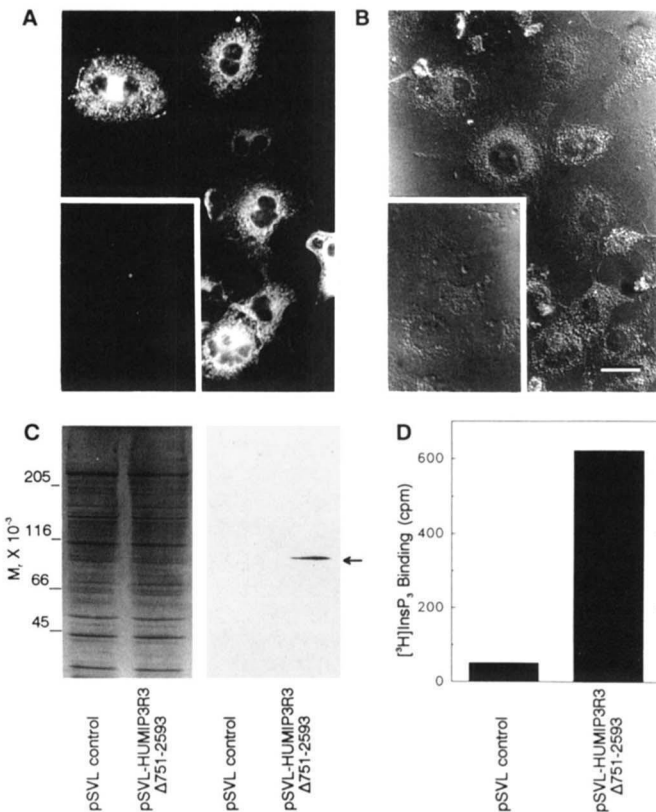


FIG. 5. Expression of the ligand binding domain of the type 3 InsP_3R in COS-7 cells. Cells were transfected with controlDNA (pSVL vector) or an expression construct (pSVL-HUMIP3R3 Δ 751–2593) which encodes the NH₂-terminal 750 residues fused to the COOH-terminal 78 residues (see Fig. 1D). *A*, immunofluorescence and *B*, Nomarsky microscopy of COS-7 cultures 48 hr post-transfection with the expression construct which have been labeled with anti-GST-H3CT antibodies followed by rhodamine-conjugated goat anti-rabbit antibodies. As shown, abundant expression of fusion protein in 80–90% of the cells was typical. Control-transfected cells did not label (*insets*). Bar, 40 μm . *C*, lysates from cells transfected with pSVL or pSVL-HUMIP3R3 Δ 751–2593 were electrophoresed (25 $\mu\text{g}/\text{lane}$) and analyzed by Coomassie Blue staining (*left panel*) and Western blotting (*right panel*). Arrow indicates the immunoreactive 90 kDa band representing the recombinant protein. *D*, specific [³H]InsP₃ binding to 100 μg lysate protein from COS-7 cells transfected with the indicated plasmids. Data are means of duplicate measurements and are representative of three separate transfections.

expression construct expressed approximately 10–12 times more specific [³H]InsP₃ binding activity than lysates from control-transfected cells (Fig. 5*D*), demonstrating that this region of cDNA encodes an InsP₃-binding domain.

To determine the specificity of InsP₃ binding in COS-7 lysates expressing the recombinant protein, inhibition experiments were performed with various inositol phosphates. Inhibition of [³H]InsP₃ binding by InsP₃ demonstrated a single, non-interacting population of binding sites with an apparent K_d of $151 \pm 20 \text{ nm}$ ($n = 3$) (Fig. 6, *A* and *B*). The order of specificity was: InsP₃ >> Ins 1,3,4,5-P₄ > InsP₆ > Ins 1,4-P₂ >> Ins 1-P (Fig. 6*A*).

Immunocytochemical Localization of Type 3 InsP_3R in Adult Rat Jejunum.—Previous *in situ* hybridization studies demonstrated high levels of type 3 InsP_3R mRNA in the fetal mouse intestine (7). Anti-GST-H3CT antibodies also recognize a single 250-kDa protein on Western blots of adult rat enterocyte homogenates (data not shown), suggesting that the rat homolog of the type 3 InsP_3R is also present in adult intestine. To localize the type 3 InsP_3R , frozen sections of adult rat jejunum were labeled with affinity-purified anti-GST-H3CT antibodies. A granular pattern of staining was apparent throughout the cytoplasm of crypt (Fig. 7*A*) and villus (Fig. 7*B*) enterocytes,

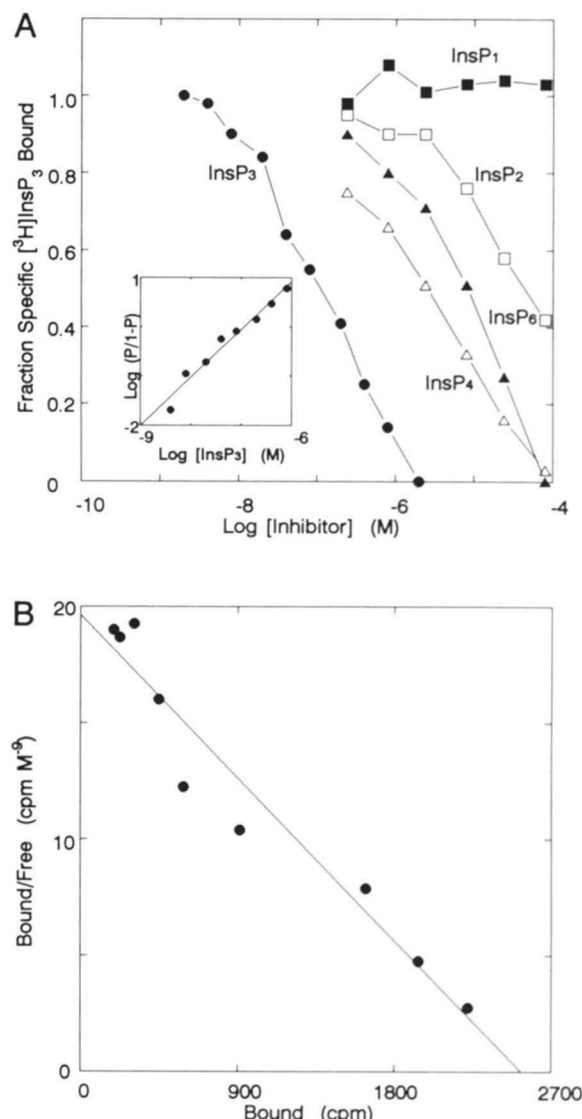


FIG. 6. Specificity of InsP_3 binding to the ligand binding domain of the type 3 InsP_3R . *A*, binding of 8 nm [³H]Ins 1,4,5-P₃ to lysates of COS-7 cells transfected with pSVL-HUMIP3R3 Δ 751–2593 was measured in the presence of various concentrations of inhibitors. *Inset*, Hill plot of the data for inhibition by Ins 1,4,5-P₃ reveals that this competition curve follows the simple Langmuir isotherm characteristic of a uniform, non-interacting population of binding sites ($n_H = 0.98$). *B*, Scatchard analysis of the competitive inhibition by InsP₃. Three separate transfections were analyzed; the results of a typical experiment are shown. The mean $K_d \pm \text{S.E.}$ ($n = 3$) is $151 \pm 20 \text{ nm}$. The mean IC_{50} values $\pm \text{S.E.}$ ($n = 3$) for other inositol phosphates were: Ins 1,3,4,5-P₄, $3.9 \pm 1.1 \mu\text{m}$; InsP₆, $15.4 \pm 6.2 \mu\text{m}$; Ins 1,4-P₂, $30.3 \pm 11.0 \mu\text{m}$.

suggesting localization on the endoplasmic reticulum. Villus enterocytes, however, exhibited more prominent staining in the cytoplasm adjacent to the apical brush border. No staining was clearly associated with nuclei or plasma membranes. Staining was specific for enterocytes: cells in the lamina propria, submucosa, and muscularis layers did not stain. Control sections treated with the same antiserum affinity-purified on a GST affinity column showed no staining (Fig. 7*C* and *D*), indicating that staining was specific for the type 3 InsP_3R COOH-terminal, not a GST-like protein.

DISCUSSION

This study describes the primary structure of a third member of the vertebrate InsP_3R gene family, the type 3 InsP_3R , deduced by sequencing cDNA clones from the human colon ad-

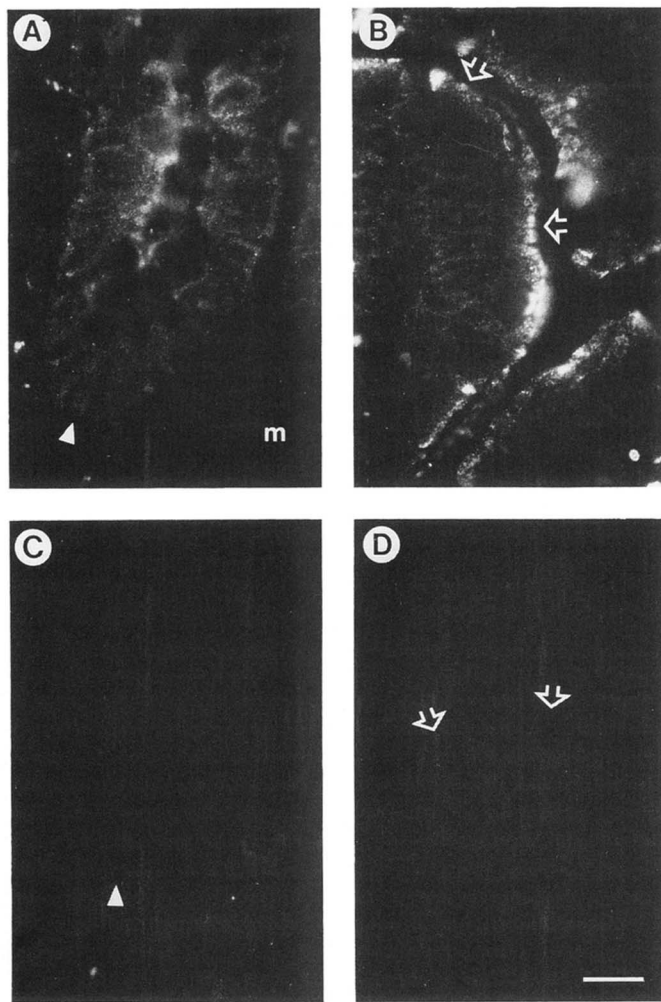


FIG. 7. Immunocytochemical localization of the type 3 InsP_3R in rat jejunal crypt and villus cells. Sections of adult rat jejunum were incubated with affinity-purified antibodies against GST-H3CT (*A*, *B*) or control antibodies against GST alone (*C*, *D*). Immunoreactive type 3 InsP_3R was visualized using rhodamine-conjugated goat anti-rabbit antiserum. *A*, crypt enterocytes showing immunoreactivity throughout the cytoplasm but excluded from nuclei. Smooth muscle cells in the muscularis layers (*m*) do not contain detectable immunoreactivity. Arrowhead points to the base of the crypt. *B*, villus enterocytes are also labeled throughout the cytoplasm but a greater concentration of immunoreactivity is adjacent to the apical surface of the cells. Arrows delimit the apical surface of a villus. *C* and *D*, crypt and villus enterocytes, respectively, incubated with the control antibodies. No staining was detectable. Arrowheads and arrows indicate similar regions as those in *A* and *B*. Bar, 20 μm .

enocarcinoma line, HT29. Previously, only a 147-amino-acid segment of this protein had been sequenced (5) and its gene, *ITPR3*, had been mapped to chromosome 6 in the region pter-p21 (32). In the present study, complete sequencing of the type 3 InsP_3R revealed that it shares considerable structural similarity with other InsP_3Rs over its entire length. InsP_3 binding activity was associated with the native protein, which was isolated by immunoprecipitation with antibodies raised against a COOH-terminal fusion protein. The ligand-binding domain was localized to the NH₂-terminal 750 amino acids by transiently expressing this region in COS-7 cells and characterizing the selectivity of binding for various inositol phosphates. Immunocytochemistry of the intestine revealed a subcellular distribution in enterocytes consistent with localization on the endoplasmic reticulum. Together, these results demonstrate that the product of the *ITPR3* gene is a genuine InsP_3R sharing similar topology, ligand-binding properties, and subcellular lo-

calization with other InsP_3Rs . Its presence and distribution in enterocytes suggest that it probably mediates InsP_3 -gated Ca^{2+} release from intracellular stores in these cells.

The differential distribution of the type 3 InsP_3R in crypt and villus enterocytes is remarkably consistent with the locations of the known Ca^{2+} effectors in these cells. In crypt cells, where Ca^{2+} activates basolateral K^+ channels (24), staining is distributed throughout the scarce cytoplasm of these cells (Fig. 7*A*). In villus cells, where Ca^{2+} inhibits Na^+/H^+ exchange across the apical membrane (26) and has been implicated in regulating cytoskeletal interactions in the brush border and terminal web (27, 28), staining is concentrated in the region of the terminal web (Fig. 7*B*). Recently, it was demonstrated that the effective range of cytosolic Ca^{2+} signaling is only 0.5 μm , due to the rapid buffering of Ca^{2+} by cytoplasm (46). In that same study, it was shown that the effective range of InsP_3 is about 20 μm . These findings could explain why the type 3 InsP_3R colocalizes with Ca^{2+} effectors in enterocytes, and how InsP_3 , which is presumably generated by humoral signals at the basal surface of the villus enterocyte, can trigger InsP_3Rs located at the other pole of the cell.

A previous PCR survey of mouse tissues detected type 3 InsP_3R mRNA in brain, lung, kidney, gastrointestinal tract, testis, thymus, spleen, and placenta; with appreciably higher levels present in the gastrointestinal tract and thymus (7). In the same report, *in situ* hybridization data was interpreted to suggest that the type 3 InsP_3R is most abundant in the smooth muscle layers of the fetal mouse intestine (7). Immunocytochemical localization in the present study confirmed the expression of type 3 InsP_3R in the adult rat gastrointestinal tract, but revealed that it is localized in the epithelial layer, not the smooth muscle layers (Fig. 7*A*, *B*). One possible explanation for this difference may be that the pattern of type 3 InsP_3R expression in the intestine changes between the fetus and adult. Alternatively, the limited resolution intrinsic to autoradiography may have given misleading results in the previous study (7).

Since the discovery of InsP_3 -gated Ca^{2+} channels in the plasma membrane of lymphocytes (47), much research has been directed at identifying plasma membrane forms of InsP_3Rs . The presence of type 3 InsP_3R mRNA in the thymus (7) suggests that the type 3 InsP_3R could represent the plasma membrane form of InsP_3R in T-lymphocytes which has recently also been localized biochemically (48) and immunologically (49). Data reported here, however, indicate that the type 3 InsP_3R exhibits different properties than the T-cell plasma membrane InsP_3R . First, antibodies against the type 3 InsP_3R do not stain the large population of lymphoid cells in the gut mucosa, many of which are T lymphocytes. Second, the pharmacology of the type 3 InsP_3R differs from that of the T lymphocyte plasma membrane InsP_3R . The InsP_3 -binding affinity of the type 3 InsP_3R ligand binding domain ($K_d = 151 \text{ nM}$) (Fig. 6*B*) resembles the affinities measured for other microsomal InsP_3Rs ($K_d = 1.9 - 300 \text{ nM}$) (reviewed in Ref. 50), whereas T cell plasma membranes exhibit low-affinity binding ($K_d = 0.8 - 1 \text{ } \mu\text{M}$) (48). Furthermore, inhibition of [³H] InsP_3 binding by $\text{InsP}_1,3,4,5-\text{P}_4$ is not nearly as effective at the type 3 InsP_3R binding site ($IC_{50} = 3.9 \text{ } \mu\text{M}$) (Fig. 6*A*) as it is at the T cell plasma membrane binding site ($IC_{50} = 600 - 800 \text{ nM}$) (48). Therefore, the type 3 InsP_3R mRNA which is present in the thymus probably does not encode the T-cell plasma membrane InsP_3R .

With the additional knowledge gained from deducing the primary structure of the type 3 InsP_3R , a common structure for all of the InsP_3R polypeptides can be proposed. As shown in Fig. 3*C* and *D*, the amino acid sequences of InsP_3Rs conform to a model containing thirteen conserved and thirteen variable regions. Table 1 lists the locations and percentages of identity of

the conserved regions for the human type 3 and rat type 1 InsP₃Rs. By analogy with other families of proteins whose structure-function relationships have been extensively studied, such as the GTPase superfamily (51), it is likely that the conserved regions of InsP₃R polypeptides represent whole or partial domains which mediate activities common to all InsP₃Rs. Variable regions, on the other hand, may represent either functionless regions which drifted in the absence of environmental selection or regions which confer differences in function among InsP₃R isoforms. While this manuscript was in preparation, the rat type 3 InsP₃R sequence was independently reported (52). Relative to the rodent sequence, the human type 3 InsP₃R contains 128 amino acid substitutions and a single amino acid insertion. The percentage of amino acid substitutions in variable regions (12.1%) is nearly four times greater than the percentage of substitutions (3.2%) in conserved regions. Therefore, just as for the products of different InsP₃R genes, most of the variable regions of these two proteins encoded by homologous genes were not subjected to the same degree of selection pressure as the conserved regions. However, three variable regions in the type 3 InsP₃R sequence, the second, fourth, and tenth regions, exhibit 100% amino acid identity between the human and rat homologs. The high degree of conservation in these regions implies that they may be areas where the type 3 InsP₃R is functionally divergent from other InsP₃R isoforms.

In addition to the type 3 InsP₃R, the human homolog of the type 1 InsP₃R was identified in homogenates of undifferentiated HT29 cells by Western blotting, and its cDNA has been partially sequenced (data not shown). The presence of type 1 as well as type 3 InsP₃Rs in HT29 cell homogenates raises questions regarding the expression and function of these isoforms in enterocytes. Are both types of InsP₃Rs coexpressed in individual cells in culture or *in vivo*? If they are coexpressed, are they located on the same intracellular Ca²⁺-storage compartments? Even when HT29 cells are cultured in the presence of glucose, a small proportion of cells differentiate into an enterocyte-like phenotype (31). Therefore, it is possible that type 1 and type 3 InsP₃Rs are differentially expressed among proliferating and differentiated cells, a hypothesis which is being tested by examining InsP₃R expression during induced differentiation of HT29 cell cultures. In the intestine, type 3 InsP₃R is present both in undifferentiated crypt cells and in terminally differentiated villus cells (Fig. 7A, B), although the level of expression appears to be greater in the villus. Studies to localize the type 1 InsP₃R in the intestinal epithelium are currently under way. Together with efforts to characterize the two intestinal InsP₃R isoforms biochemically, these studies will help to define the roles of these receptors in enterocytes.

Acknowledgments—I thank N. E. Simister for the HT29 cDNA library, P. DeCamilli for the antiserum to the type 1 InsP₃R, R. C. Nakisa for the program DOTPLOT, and C. Korsgren, T. D. Gilmore, and C. M. Cohen for expert technical advice.

REFERENCES

- Berridge, M. J., and Irvine, R. F. (1989) *Nature* **341**, 197–205
- Furuichi, T., Yoshikawa, S., Miyawaki, A., Wada, K., Maeda, N., and Mikoshiba, K. (1989) *Nature* **342**, 32–38
- Mignery, G. A., Newton, C. L., Archer, B. T., III, and Sudhof, T. C. (1990) *J. Biol. Chem.* **265**, 12679–12685
- Kume, S., Muto, A., Aruga, J., Nakagawa, T., Michikawa, T., Furuichi, T., Nakade, S., Okano, H., and Mikoshiba, K. (1993) *Cell* **73**, 555–570
- Sudhof, T. C., Newton, C. L., Archer, B. T., III, Ushkaryov, Y. A., and Mignery, G. A. (1991) *EMBO J.* **10**, 3199–3206
- Yoshikawa, S., Tanimura, T., Miyawaki, A., Nakamura, M., Yuzaki, M., Furuchi, T., and Mikoshiba, K. (1992) *J. Biol. Chem.* **267**, 16613–16619
- Ross, C. A., Danoff, S. K., Schell, M. J., Snyder, S. H., and Ullrich, A. (1992) *Proc. Natl. Acad. Sci. U. S. A.* **87**, 3841–3845
- Danoff, S. K., Ferris, C. D., Donath, C., Fischer, G. A., Munemitsu, S., Ullrich, A., Snyder, S. H., and Ross, C. A. (1991) *Proc. Natl. Acad. Sci. U. S. A.* **88**, 2951–2955
- Nakagawa, T., Okano, H., Furuichi, T., Aruga, J., and Mikoshiba, K. (1991) *Proc. Natl. Acad. Sci. U. S. A.* **88**, 6244–6248
- Supattapone, S., Danoff, S. K., Theibert, A., Joseph, S. K., Steiner, J., and Snyder, S. H. (1988) *Proc. Natl. Acad. Sci. U. S. A.* **85**, 8747–8750
- Ferris, C. D., Huganir, R. L., Bredt, D. S., Cameron, A. M., and Snyder, S. H. (1991) *Proc. Natl. Acad. Sci. U. S. A.* **88**, 2232–2235
- Ferris, C. D., Huganir, R. L., and Snyder, S. H. (1990) *Proc. Natl. Acad. Sci. U. S. A.* **87**, 2147–2151
- Maeda, N., Kawasaki, T., Nakade, S., Yokota, N., Taguchi, T., Kasai, M., and Mikoshiba, K. (1991) *J. Biol. Chem.* **266**, 1109–1116
- Yada, T., Oiki, S., Ueda, S., and Okada, Y. (1989) *J. Membr. Biol.* **112**, 159–167
- Chang, E. B., and Musch, M. W. (1990) *Life Sci.* **46**, 1913–1921
- Dickinson, K. E., Frizzell, R. A., and Sekar, M. C. (1992) *Eur. J. Pharmacol.* **225**, 291–298
- Bozou, J. C., Rochet, N., Magnaldo, I., Vincent, J. P., and Kitabgi, P. (1989) *Biochem. J.* **264**, 871–878
- Lieberherr, M., Grosse, B., Duchambon, P., and Drueke, T. (1989) *J. Biol. Chem.* **264**, 20403–20406
- Sjolander, A., Gronroos, E., Hammarstrom, S., and Andersson, T. (1990) *J. Biol. Chem.* **265**, 20976–20981
- Velasco, G., Shears, S. B., Michell, R. H., and Lazo, P. S. (1986) *Biochem. Biophys. Res. Commun.* **139**, 612–618
- VanCorven, E. J., Verboost, P. M., deJong, M. D., and vanOs, C. H. (1987) *Cell Calcium* **8**, 197–206
- Sepulveda, F. V., and Smith, S. M. (1987) *Pfluegers Arch.* **408**, 231–238
- Ilundain, A., O'Brien, J. A., Burton, K. A., and Sepulveda, F. V. (1987) *Biochim. Biophys. Acta* **896**, 113–116
- Walters, R. J., and Sepulveda, F. V. (1991) *Pfluegers Arch.* **419**, 537–539
- Morris, A. P., and Frizzell, R. A. (1993) *Am. J. Physiol.* **264**, C968–C976
- Cohen, M. E., Reinlib, L., Watson, A. J., Gorelick, F., Rys-Sikora, K., Tse, M., Rood, R. P., Czernik, A. J., Sharp, G. W., and Donowitz, M. (1990) *Proc. Natl. Acad. Sci. U. S. A.* **87**, 8990–8994
- Matovcik, L. M., Haimowitz, B., Goldenring, J. R., Czernik, A. J., and Gorelick, F. S. (1993) *Am. J. Physiol.* **264**, C1029–C1036
- Swanljung-Collins, H., and Collins, J. H. (1992) *J. Biol. Chem.* **267**, 3445–3454
- Fogh, J., and Trempe, G. (1975) in *Human Tumor Cells in vitro* (Fogh, J., ed) pp. 115–141, Plenum Press, New York
- Rousset, M. (1986) *Biochimie* **68**, 1035–1040
- Pinto, M., Appay, M. D., Simon-Assmann, P., Chevalier, G., Dracopoli, N., Fogh, J., and Zweibaum, A. (1982) *Biol. Cell.* **44**, 193–196
- Ozelik, T., Sudhof, T. C., and Francke, U. (1991) *Cytogenet. Cell Genet. Abstr.* **58**, 1880
- Sanger, F., Nicklen, S., and Coulson, A. R. (1977) *Proc. Natl. Acad. Sci. U. S. A.* **74**, 5463–5467
- Laemmli, U. K. (1970) *Nature* **227**, 680–685
- Towbin, H. T., Staehelin, T., and Gordon, J. (1979) *Proc. Natl. Acad. Sci. U. S. A.* **76**, 4350–4354
- Kozak, M. (1987) *Nucleic Acids Res.* **15**, 8125–8148
- Klein, P., Kanehisa, M., and DeLisi, C. (1985) *Biochim. Biophys. Acta* **815**, 468–476
- Rao, J. K. M., and Argos, P. (1986) *Biochim. Biophys. Acta* **869**, 197–214
- Ferris, C. D., Cameron, A. M., Bredt, D. S., Huganir, R. L., and Snyder, S. H. (1991) *Biochem. Biophys. Res. Commun.* **175**, 192–198
- Feramisco, J. R., Glass, D. B., and Krebs, E. G. (1980) *J. Biol. Chem.* **255**, 4240–4245
- Woodget, J. R., Gould, K. L., and Hunter, T. (1986) *Eur. J. Biochem.* **161**, 177–184
- Colbran, R. J., Schworer, C. M., Hashimoto, Y., Fong, Y. L., Rich, D. P., Smith, M. K., and Soderling, T. R. (1989) *Biochem. J.* **258**, 313–325
- Matsudaira, P. (1987) *J. Biol. Chem.* **262**, 10035–10038
- Mignery, G. A., and Sudhof, T. C. (1990) *EMBO J.* **9**, 3893–3898
- Miyawaki, A., Furuichi, T., Ryuu, Y., Yoshikawa, S., Nakagawa, T., Saitoh, T., and Mikoshiba, K. (1991) *Proc. Natl. Acad. Sci. U. S. A.* **88**, 4911–4915
- Allbritton, N. L., Meyer, T., and Stryer, L. (1992) *Science* **258**, 1812–1814
- Kuno, M., and Gardner, P. (1987) *Nature* **326**, 301–304
- Khan, A. A., Steiner, J. P., and Snyder, S. H. (1992) *Proc. Natl. Acad. Sci. U. S. A.* **89**, 2849–2853
- Khan, A. A., Steiner, J. P., Klein, M. G., Schneider, M. F., and Snyder, S. H. (1992) *Science* **257**, 815–818
- Taylor, C. W., and Richardson, A. (1991) *Pharmacol. Ther.* **51**, 97–137
- Bourne, H. R., Sanders, D. A., and McCormick, F. (1991) *Nature* **349**, 117–127
- Blondel, O., Takeda, J., Janssen, H., Seino, S., and Bell, G. I. (1993) *J. Biol. Chem.* **268**, 11356–11363
- Kyte, J., and Doolittle, R. F. (1982) *J. Mol. Biol.* **157**, 105–132